APPLICATION OF PASSIVE AND ACTIVE DAMPING TECHNIQUES TO THE PACOSS REPRESENTATIVE SYSTEM

Daniel R. Morgenthaler
Martin Marietta Astronautics Group
Denver, Colorado 80201

ABSTRACT

This paper presents the results of a study performed on the Passive and Active Control of Space Structures (PACOSS) Representative System Article (RSA). The RSA is a representative large space structure (LSS) with optical components inherent in its design. The study examines methods of achieving a performance goal for a slew maneuver of the RSA generated by an attitude control system. In order to achieve a prescribed goal for the slew, damping is added to the flexible structural modes. Two damping approaches are considered: active control alone, and the passive/active damping design approach utilized on the PACOSS program. Quantitative estimates of the properties of the damped systems generated using the two approaches are compared. The passive/active approach is seen to result in a much more efficient overall system design. Even using assumptions which favor the active control component, the passive/active design methodology resulted in nearly 25% less added weight due to active and/or passive control measures. Also, a 97% savings in active control energy, and a simpler and more reliable overall system were achieved.

INTRODUCTION

Future military and civilian space systems will typically be very large but lightweight. These characteristics lead to dense modal spectra at low frequencies which often will overlap attitude control bandwidths. The mission profiles of these systems also require low vibration levels of critical components in order to meet mission goals. The PACOSS RSA design (Figure 1) is based on a survey of planned and conceptual space systems required to meet specific mission objectives. This survey revealed extensive requirements for relatively large, lightweight structures possessing the ability for precise pointing and, in some instances, rapid retargeting. The survey included consideration of both military and civilian system concepts, and disturbances affecting such systems. Further details of the mission survey, RSA configuration, and system design are given in several publications (References 1,2,3).

The configuration of the RSA is not mission specific but a representation of several missions and requirements in one system. The RSA reflects the mission requirements of first generation LSS, and it is assumed that its mission would utilize the reflecting surfaces inherent in its design in an optical, infrared, or communication system. The analysis and design results, therefore, are representative of systems with similar reflecting components and other systems with requirements for vibration control.

There are essentially two design methodologies which can be used to reduce structural vibrations: active control and passive damping. This study examines the system properties following application of active damping to the RSA using velocity feedback and also following application of both passive and active damping in an integrated methodology. A summary of the methodology is given in Reference 4.

The RSA is a symmetric structure, facilitating uncoupled control systems for pitch and roll-yaw motions. This study considered only symmetric (pitch) dynamics, and damping design was only considered for modes which degrade slew

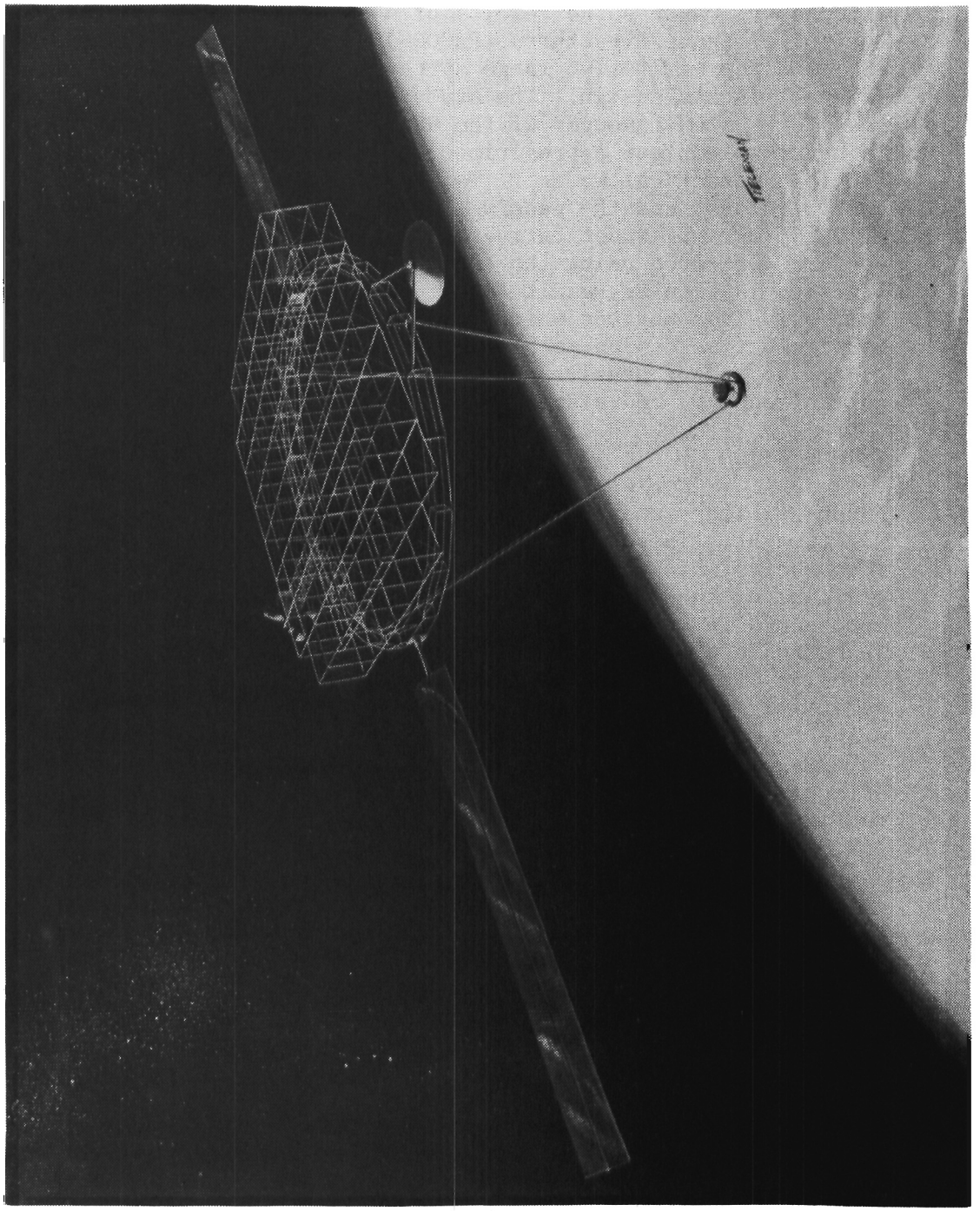

Figure 1 - PACOSS Representative System (RSA)

KCD-2

performance for this axis. The methodology and results would be similar if roll-yaw dynamics were considered.

RSA Configuration and Performance Measure

The RSA consists of seven substructures, each with a specific function to perform to meet mission goals. Table 1 contains a description of the various components and future systems to which these substructures are traceable. The sizes of components can be considered representative of a typical spacecraft. Weight and stress constraints were not considered, but strain energy distributions were adjusted to produce a reasonably weight efficient design while accommodating passive damping treatments.

Table 1 - RSA Component Overview

COMPONENT	DIMENSION (m)	MASS (kg)	FUNCTION	APPLICABLE SYSTEMS
1) Box Truss	20x20x2.5	2295	Primary reflecting surface support and/or spacecraft subsystem carrier	Space Based Radar Large Earth Observing System Mobile Communications Satellite Space Station
2) Ring Truss	Diameter: 22.4	1113	Central support hub: ties system component together	Generic Truss Structure
3) Tripod	Diameter of Base: 20 Height: 20	840	Secondary reflecting surface support	Space Based Laser Large Deployable Reflector
4) Equip. Platform	Length: 10	2634	Support/isolate sensitive equipment or experiments away from main structure	Space Station Strategic Defense Initiative (SDI)
5) Antenna	Diameter: 5	345	Earth communications: command and control	Space Base Radar Space Station Satellites
6, Solar 7) Arrays	Length: 20	786	Power generation, sized for 20 kW	Space Based Radar Space Station Satellites

A Cassegrain optical system is contained in the baseline RSA design, consisting of reflecting surfaces located on box truss and tripod structures. Of primary interest to the overall performance of this system is the instantaneous pointing angle of the optical system or line-of-sight (LOS). The mathematical definition of the LOS is given in Figure 2. The LOS is written relative to the rotation of a reference sensor in this definition.

RSA Performance Goal and Attitude Control System

The major disturbance source for the RSA was assumed to be a maneuvering of the vehicle in order to repoint the optical system. The torques necessary to slew the spacecraft were generated by an attitude control system using four torque wheels mounted on the structure. The design of the attitude control was concieved to be simple but characteristic of those which will be used on first generation LSS. The attitude control system is discussed in detail in Reference 2. The disturbance source considered was a small angle slew (0.01 rad) generated by the attitude control.

The attitude control system uses angular rate and position feedback to eliminate pointing errors relative to a target angle. The control design consisted of selecting feedback gains and filter characteristics to achieve acceptable closed-loop slew performance which while minimizing structural vibration and remaining within slew acceleration limits. These parameters for the control system are included on Figure 3, along with the attitude control actuator locations and a block diagram. The resulting closed-loop rigid body frequency and damping were approximately 0.50 Hz and 0.707, respectively.

The baseline system also included an actuator to control the secondary mirror angle which was gimballed from its support structure on the tripod. Feedback gains were selected such that the closed-loop frequency and damping of the mode consisting of rotation of the secondary mirror on its support were 0.50 Hz and 0.707, respectively. These gains produced acceptable response of the mirror for slew maneuvering while uncoupling mirror rotation from higher frequency disturbances.

The figure of merit utilized for evaluation of the system's performance for the slew maneuver was settling time. This is a measure of the time required for the system to return to a state where it may operate satisfactorily following the transient disturbance. For spacecraft slew maneuvers, typically a maximum angular acceleration is available (or allowable) and fast settling time following conclusion of the maneuver is the goal. For the RSA, 0.1 rad/sec^2 was considered as the angular acceleration limit. The goal under for the slew maneuver was to settle within 1.0 second of maneuver completion to below a 50 micro-rad error to target. A summary of the slew maneuver and performance goals are included in Table 2.

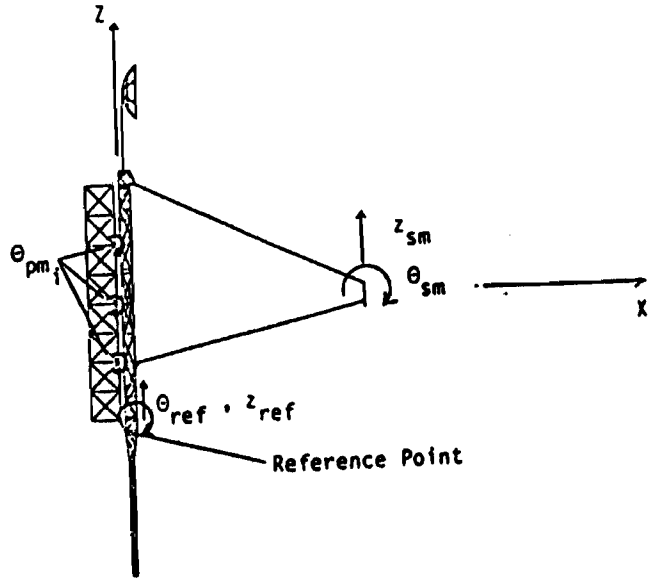

$$LOS_y = \left(2\frac{f_s}{f_p} - 1\right)\theta_{ref} + \frac{2}{13}\sum_{i=1}^{13}\theta_{pm_i} - 2\frac{f_s}{f_p}\theta_{sm} - \frac{1}{f_p}(z_{ref} - z_{sm})\ flex$$

Where,

f_s = Focal length of secondary mirror

f_p = Focal length of primary mirror

$(z_{ref} - z_{sm})_{flex}$ = Relative z deflection of secondary mirror to reference point due to structural deformation

NOTES:

Sum over θ_{pm_i} represents an average primary mirror deformation

LOS about z-axis has sign change on relative translation term;

$$-\frac{1}{f_p}(z_{ref} - z_{sm})_{flex} \Rightarrow +\frac{1}{f_p}(y_{ref} - y_{sm})_{flex}$$

Relative LOS is defined as : Inertial LOS - Rigid Body Motion

Figure 2 - LOS Mathematical Definition

Table 2 - RSA Performance Goals for Slew

DISTURBANCE	DISTURBANCE VALUES	GOAL FOR PERFORMANCE
Spacecraft slew maneuver	0.01 rad slew with 0.1 rad/sec² maximum angular acceleration	Pointing error settle to within 50 μrad within 1 sec of slew completion

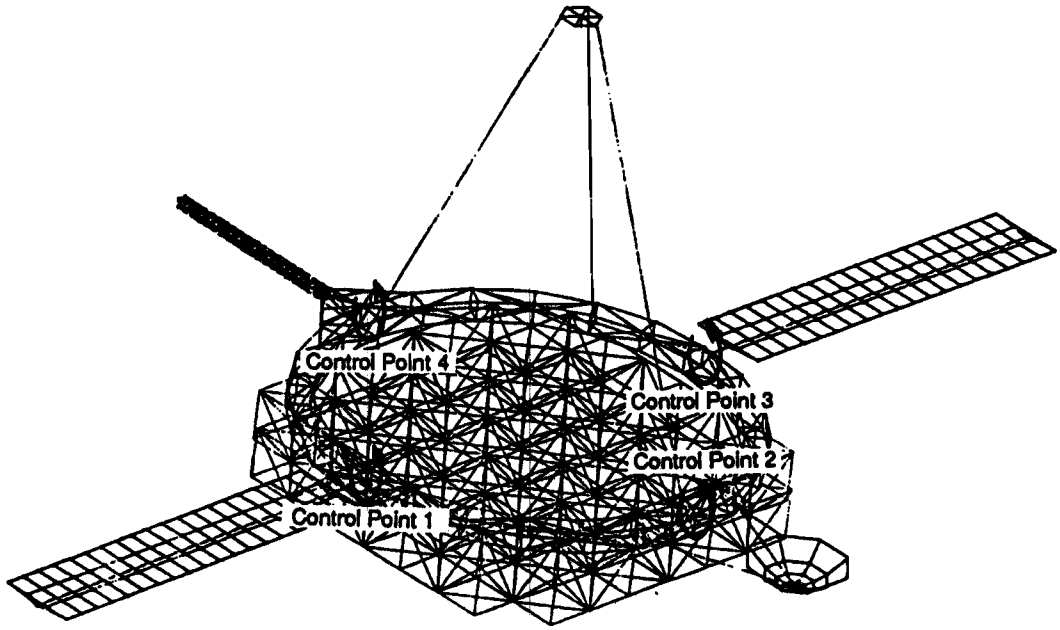

Note: Inertial reference sensor is located at Control Point 4

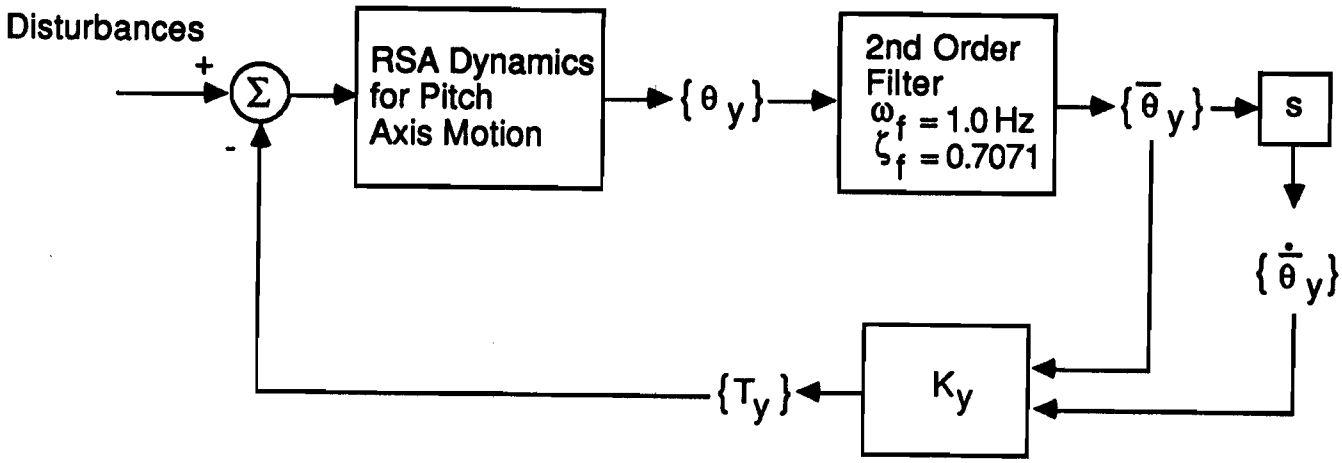

$$\{T_y\} = \begin{bmatrix} 2.12 \times 10^6 & 1.91 \times 10^6 \end{bmatrix} \begin{Bmatrix} \bar{\theta}_y \\ \dot{\bar{\theta}}_y \end{Bmatrix}$$

where:

T_y = attitude control torque (1/4 of this applied at each control point)

θ_y = pitch target angle error at reference sensor

$\bar{\theta}_y$ = filtered angle error signal

$\dot{\bar{\theta}}_y$ = filtered angle error signal rate

Figure 3 Attitude Control System Block Diagram and Torque Wheel Locations

RSA Baseline Model

Analysis of the RSA system required a model of the structure and associated hardware. Passive damping analysis required a relatively detailed finite element model to allow subsequent Modal Strain Energy (MSE) distribution calculations. The finite element modeling and analysis was performed using the MSC/NASTRAN program.

Component mode synthesis was used to compute the frequencies, mode shapes and strain energy distribution of the RSA model. A total of 210 system modes were found to be present in the frequency range of interest (0-10 Hz). Many of these modes involve local solar array motion at very low frequencies. System modes which are global in character are likely to be important in attitude control and performance evaluation. A relatively high number of RSA system modes are global; that is, several components possess significant kinetic and potential (strain) energy in a given system mode. This characteristic of the RSA, and future LSS, will complicate the control design process.

Candidate passive damping treatments and member sets to be damped were selected during the modeling process, and these are given in Table 3. The final member sizes are such that high strain energy is contained in the selected member sets for global system modes. From the strain energy distributions in these global modes it was apparent that modes with high box truss participation possessed a high percentage of strain energy in the diagonals. Similarly, modes with high tripod participation had high energy in the tripod legs. These distributions allowed for the efficient application of passive damping treatments to damp these important global modes.

Table 3 - Selected Component Damping Treatment Types

COMPONENT	POSSIBLE TREATMENTS
Box Truss	Extensional shear damper with static load capability (diagonals)
Ring Truss	None
Tripod	Constrained layer treatment (legs)
Equipment Platform	Extensional shear damper (diagonals)
Antenna	Constrained layer treatment (legs)
Solar Arrays	Constrained layer treatment (blanket hinge lines)

Baseline Structural Performance

In order to determine the performance of the baseline system and also modes requiring passive or active damping, a slew maneuver of the system was simulated. The modes which could couple significantly with the attitude control were selected for use in the analysis, as were flexible modes which were important for LOS analysis. The modal LOS was calculated using the definition of the LOS and the values of the translations and rotations of the appropriate points in the mode shapes.

Closed-loop poles for the flexible system coupled to the previously described control system were calculated assuming 0.2% modal viscous damping (a damping level characteristic of precision large space structures), and including 25 flexible modes. Table 4 lists the natural frequencies and damping ratios of the baseline closed-loop system including these modes. The effects of truncation were examined, and these modes were determined to be a sufficient set to characterize spillover and coupling between the attitude control system while providing accurate LOS simulation.

Because the closed loop system was unstable, the open-loop damping levels of those modes which were driven unstable (modes 129,158, and 201) were increased to a level such that the closed loop damping of these modes was the nominal value of 0.2%. This system was used to compute the nominal performance. The slew response of the stabilized closed loop system for a pitch axis maneuver was generated and is given in Figure 4. Notice that the response involves several modes and has a lengthy settling time. The time to complete the slew maneuver if the RSA were a rigid body is approximately 3.25 seconds. After 1.0 seconds following the rigid body maneuver time, the baseline system "settles" to within an error of 4.5×10^{-4} radians as shown in the figure. This exceeds the goal level of 50 micro-radians by a factor of 10. The time required for this system to settle to the 50 micro-radian level is approximately 230 seconds.

Required Damping and Achievable Passive Damping Estimates

The damping levels required to meet the design goals for the slew maneuver may be selected in many different ways, which will in general result in damping the various modes to differing levels. For this study, damping levels based on modal settling times were used.

In order to calculate the required damping ratios for each mode, the LOS response of the system was decomposed into its various modal contributions. The settling time for the individual modes was taken to be the time required for the amplitude of the modal response to fall below the error bound of 50 micro-radians. As a preliminary step in determining the required damping levels, the attitude control torque as a function of time for a rigid RSA was generated and applied to the open loop RSA. Similarly, modal settling times were calculated for the nominal system with the attitude control loop closed. Table 5 contains a list of the modes with individual settling times greater than the settling time of 1.0 sec for these two cases.

Table 4 Natural Frequencies and Damping Values for Nominal System With Attitude Control Loop Closed

SYSTEM	OPEN LOOP		CLOSED LOOP	
MODE #	f_n (Hz)	ζ (%)	f_n (Hz)	ζ (%)
Rigid Body	0	0	0.46	60.1
Filter	1.0	70.7	0.54	81.3
7	0.01	0.2	0.50	70.7
21	0.69		0.65	0.22
23	0.73		0.77	1.72
30	1.02		0.96	1.45
32	1.02		1.02	0.20
44	1.50		1.49	0.62
48	1.53		1.51	0.75
118	2.72		2.72	0.20
124	2.78		2.78	0.45
129	2.86		2.87	-0.15
158	4.03		4.04	-0.05
165	4.21		4.22	0.17
176	4.38		4.38	0.20
182	4.55		4.55	0.16
185	5.11		5.12	0.08
187	5.68		5.68	0.16
188	5.81		5.81	0.20
191	6.45		6.45	0.10
192	6.49		6.49	0.20
196	6.96		6.96	0.18
198	7.15		7.15	0.18
199	7.31		7.31	0.15
201	7.38		7.38	-0.10
206	8.77		8.77	0.02
209	9.53	0.2	9.53	0.02

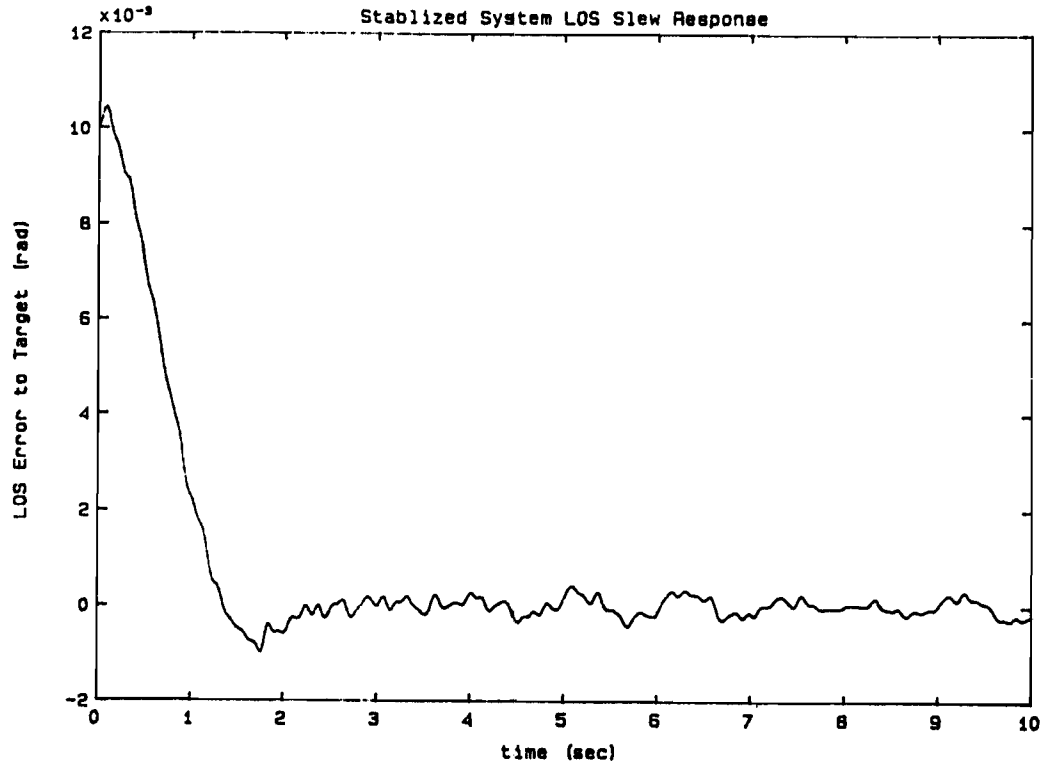

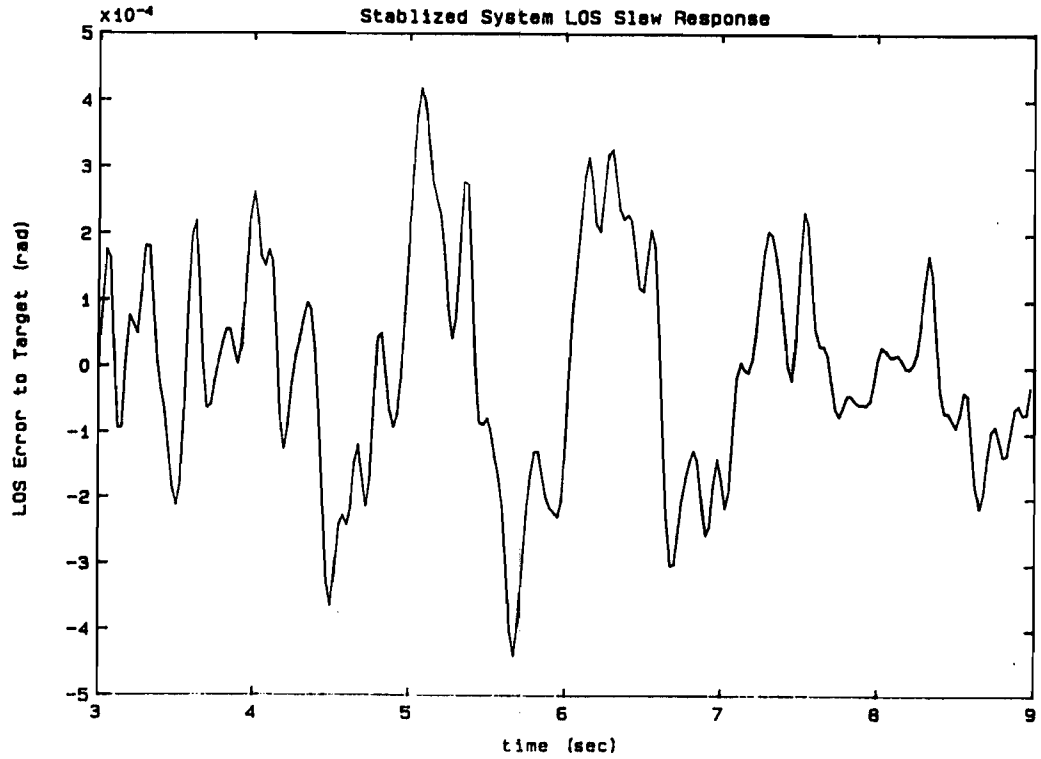

Figure 4 - Baseline System LOS Slew Response

Table 5 - Modes with High Settling Time for Baseline System

SYSTEM MODE NO.	SETTLING TIME FOR RIGID RSA TORQUE (sec)	SETTLING TIME FOR STABILIZED BASELINE CLOSED-LOOP SYSTEM (sec)
30	357	244
23	326	174
32	171	84
124	84	73
129	75	68
158	48	49
185	24	26
201	20	24
209	11	14
48	7	5
21	6	0
191	5	3
187	5	4
199	3	8
206	2	3

To find preliminary damping levels for each individual mode, the damping levels were determined so that each mode settle to within the 50 micro-radians minus a margin to allow for the addition of other modal responses at their corresponding phase angles. The modal damping values which caused the individual modes to meet the settling criterion value were calculated by iteration.

Because the responses of modes which are controllable and observable by the attitude control alter the control torque, the response of any mode was dependent on the damping of all other modes. To include these effects, the attitude control system was coupled to the flexible system using the damping levels selected as explained previously. The damping levels were then iteratively adjusted such that the closed-loop modal settling times were equal for all modes requiring damping augmentation, and the system response just met the performance goals.

The required damping levels for the targeted modes based on the above criterion are included in Table 6. Notice that there are two low frequency modes (modes 23 and 30) which are within the controller bandwidth that require high damping levels, and many modes which require low levels of damping augmentation. The modes which require high damping augmentation and have high modal settling times are the system target modes (modes 23, 30, 32, 124, 129, 158, 185, 201, and 209). These modes were specifically targeted for damping augmentation. Modes which require only low damping levels can be considered the observable modes. Most of these modes do not

Table 6 - Modal Damping Levels Selected for Modes with High Settling Time

Mode No.	Freq. (Hz)	Req'd. (%)
23	0.73	11.0
30	1.02	12.0
32	1.03	3.0
48	1.53	1.0
124	2.8	4.0
129	2.9	4.0
158	4.0	2.5
165	4.2	1.0
182	4.5	1.0
185	5.1	2.0
187	5.7	1.0
191	6.5	1.0
196	7.0	1.0
198	7.1	0.5
199	7.3	0.5
201	7.4	1.5
206	8.8	1.0
209	9.4	1.5

have settling values above the goal, but their responses are large enough when undamped that they can add with the targets to produce a slew response which does not meet the goal. The damping levels given in Table 6 imply that passive damping could greatly benefit the system, as only low to moderate levels of damping are required for a majority of the system modes.

The passive damping which may be designed into the structure using the treatments on Table 3 can be found using the modal strain energy method. In order to facilitate estimates, the modal strain energy method was utilized in the form:

$$n_j = \sum_{i=1}^{nms} n_i * \%SE_{ij} * DEF_i$$

where:

n_j = modal loss factor for jth mode
$\%SE_{ij}$ = % strain energy in ith set of damped members in jth mode
DEF_i = Assumed damping efficiency factor of ith set of damped members. Defined as the ratio of strain energy in viscoelastic used in treating the member to total member energy.
nms = # of damped member sets

Representative damping efficiencies based on the treatment types, and experience using similar treatments on the PACOSS Dynamic Test Article (DTA) were used in the estimates (Reference 4). The DTA is a scale model of the RSA.

The calculated damping of the target modes based on assumed damping efficiencies and the modal strain energy distribution using these treatments was calculated assuming a viscoelastic loss factor of 0.7, which roughly corresponds to the value of the loss factor for acrylic foam tape at 1.0 Hz and 70 F. The damping attributable to treatment of the various components is given in Table 7, along with the maximum achievable damping using these treatments.

Notice that the required damping for all target modes may be obtained using the selected treatments except for system modes 23 and 30. This table shows that by applying treatments to damp the low frequency target modes, significant damping can be achieved in the higher frequency targets and observable modes. This "passive damping spillover" is an attractive benefit found in passive damping design.

Table 7 - Maximum Achievable Damping from Treatments by Component

			Achievable Modal Damping (%)					
Req'd. (%)	Mode No.	Freq. (Hz)	Box Truss Diagonals	Tripod Legs	Equipment Platform Diagonals	Antenna Legs	Solar Array Hinges	Total
11.0	23	0.73	-	0.3	0.6	2.5	0.2	3.6
12.0	30	1.02	-	0.2	3.3	1.2	1.1	5.8
3.0	32	1.03	-	-	1.1	0.3	3.5	4.9
1.0	48	1.53	-	0.7	2.7	0.4	0.4	4.2
4.0	124	2.8	1.9	3.6	-	0.13	-	5.6
4.0	129	2.9	22.7	0.13	0.14	-	-	23.0
2.5	158	4.0	3.0	1.1	-	0.4	-	4.5
1.0	165	4.2	0.53	3.6	-	0.13	-	4.3
1.0	182	4.5	1.1	4.1	-	-	-	5.2
2.0	185	5.1	3.1	0.09	-	1.2	-	4.4
1.0	187	5.7	9.2	1.5	-	0.53	-	11.2
1.0	191	6.5	1.7	0.11	12.3	0.43	-	14.5
1.0	196	7.0	23.7	0.19	0.42	-	-	24.3
0.5	198	7.1	18.4	0.83	-	0.21	-	19.4
0.5	199	7.3	20.3	0.14	1.3	-	-	21.7
1.5	201	7.4	7.6	0.39	2.9	0.22	-	11.1
1.0	206	8.8	11.6	1.5	0.42	0.21	-	13.7
1.5	209	9.4	25.8	0.04	0.22	-	-	26.1

Control System Evaluation for Various Passive Levels

With the required modal damping levels known, a trade was examined between actively and passively achieving these levels. This trade allowed a reasonable selection of the mix of the two damping approaches based on the power requirements for the actuators and relative ease with which the required level of passive or active control could be incorporated.

In order to determine the effect of the passive and active damping levels on the system, an active control system was designed for various percentages of the maximum achievable passive damping levels given in Table 7. For example, a passive level of 50% achievable damping may be selected; this corresponds to using damping values of one-half those in the final column of Table 7. An active control system was then designed which augmented the target mode damping levels to the required levels. As the active and passive damping add approximately linearly for the levels of damping considered, the active damping was simply the difference between the required and passive damping levels. Eleven cases were considered, with percentages of achievable damping ranging from 0% to 100% by steps of 10%.

The active control algorithm implemented in each case was a form of modal space control using colocated sensors and actuators. The use of velocity feedback with colocated sensors and actuators gives an unconditionally stable system (assuming ideal sensors and actuators). However, observation and control spillover effects can seriously degrade closed-loop performance. In order to avoid spillover into the rigid body mode, the algorithm was cast such that only relative velocities were sensed and the sensor signal was the relative angular velocity between each vibration control sensor point and the reference attitude control sensor located on the ring truss. A torque was applied at the attitude control system reference point which exactly negated the torques applied at the vibration control points, so that zero net torque was applied to the system. The feedback gain matrix is thus given by:

$$K = - \phi_c^{-T} [2\zeta\omega_c] \phi_c^T$$

where ϕ_c is the relative open-loop modal matrix and $[2\zeta\omega_c]$ is the desired diagonal active modal damping matrix for the controlled modes. Note that there must be as many sensor/actuator pairs as controlled modes in this approach.

Efficient sensor/actuator pair locations were selected through consideration of over 300 candidate locations, and the points making the determinant of the ϕ_c matrix a maximum for the modes requiring damping were selected in each case.

The active control was then implemented through the following relation:

$$u_c = K y_{rel}$$

and the closed-loop system was generated using the state-space form of the flexible RSA.

For no passive damping augmentation, active control of the nine target modes was required. These modes were selected for active control since they require the highest damping, and when considered separately each had a LOS settling time which violated the performance goal. Actuator gains were determined, and the closed-loop system poles were calculated. Due to spillover the required damping was not achieved using the results of the first gain calculation, so the damping levels used in the gain calculations were iteratively adjusted to achieve closed-loop damping equal to the desired level in each controlled mode. The actuator locations selected to control these modes are identified in Figure 5. Actuators which are in symmetric pairs were considered a single actuator in the gain calculation, since only symmetric modes were considered in the analysis.

Table 8 contains the closed-loop frequencies and damping of the actively controlled system without passive damping augmentation. Notice that spillover effects due to those modes which were not considered in the gain calculation resulted in increased damping in those modes which were not targeted for active control.

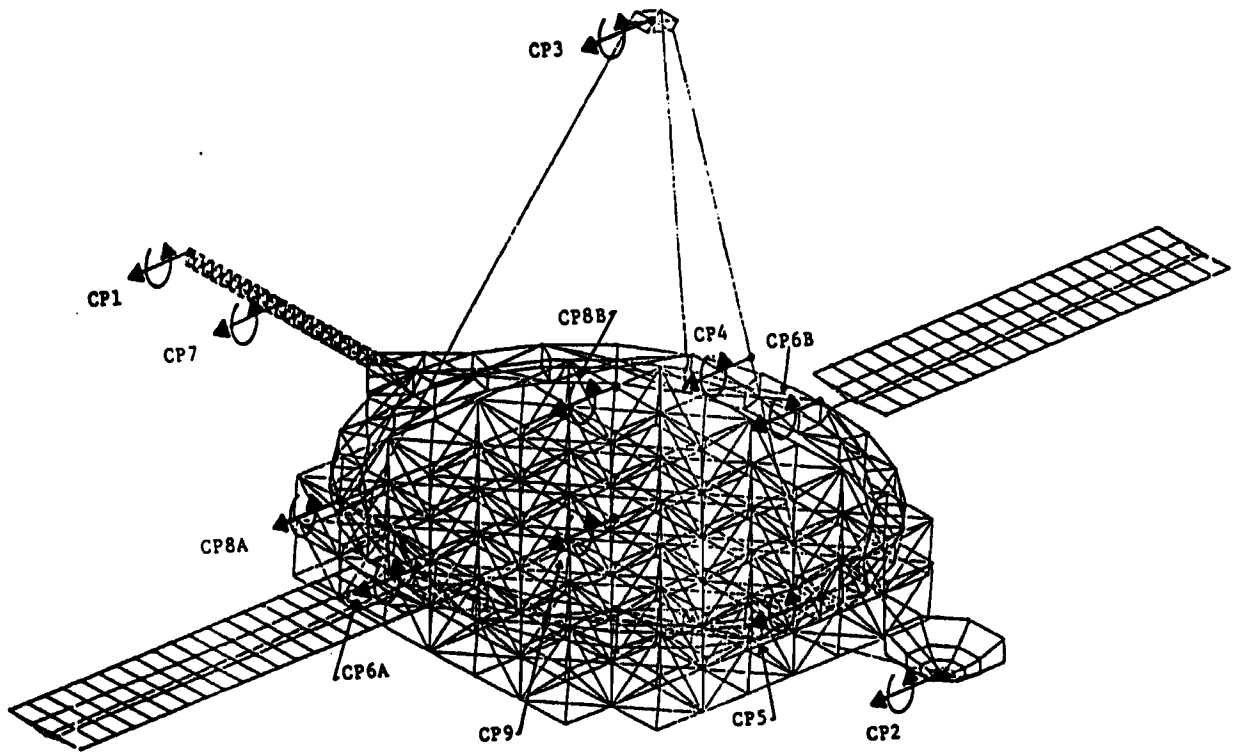

Figure 5 - Sensor/Actuator Locations for Modal Control

Table 8 - Closed-Loop Frequencies and Damping of Controlled System Without Passive Damping

SYSTEM	OPEN LOOP		CLOSED LOOP	
MODE #	f_n (Hz)	(%)	f_n (Hz)	(%)
Rigid Body	0	0	0.46	51.3
Filter	1.0	70.7	0.50	93.5
7	0.01	0.2	0.50	70.61
21	0.69		0.69	0.32
* 23	0.73		0.79	11.64
* 30	1.02		0.96	13.5
* 32	1.02		1.02	0.21
44	1.50		1.50	0.20
48	1.53		Overdamped	
118	2.72		2.72	0.23
*124	2.78		2.80	4.3
*129	2.86		2.85	4.0
*158	4.03		4.04	2.73
165	4.21		4.40	2.4
176	4.38		4.37	0.46
182	4.55		4.40	2.4
*185	5.11		5.09	2.0
187	5.68		5.8	3.0
188	5.81		5.81	0.25
191	6.45		Overdamped	
192	6.49		6.58	6.35
196	6.96		6.96	1.52
198	7.15		7.26	0.77
199	7.31		7.44	0.77
*201	7.38		7.36	1.6
206	8.77		Overdamped	
*209	9.53	0.2	9.53	1.63

*Denotes active control target mode

System mode 32, which is a mode involving torsion of the solar array blanket out of phase with motion of the main structure, requires damping but was nearly uncontrollable using reasonable actuator locations. Even though high damping levels were used for this mode in the gain calculation, the required closed-loop damping could not be achieved due to spillover. To actively damp this mode effectively would require actuators located on the flexible and lightweight solar array blankets. It was found that by using 6.0% active damping in the gain calculation for mode 32, the performance of this mode was equivalent to the 3.0% passively damped case due to coupling with other modes. Therefore, when active control of mode 32 was needed, 6.0%

damping was always used in the gain calculation. The closed-loop damping in all other modes was adjusted to be above the required level but not greater than 1.15 the required level. This factor resulted in a reasonable number of iterations to achieve the gains, while achieving active control damping levels which were at most slightly higher than necessary.

Increases in the passive damping allowed fewer modes to be actively controlled. The addition of passive damping also resulted in lower gains to control the modes which still required active damping. The active system used in each case was similar to the modal space control previously described, where the control gains were selected based on the modes still requiring active augmentation and the required active augmentation levels. The required number of actuators for each case are given in Table 9.

In order to compare the performance of the controlled systems, the LOS slew responses of the 11 cases were plotted on the same graph. This is given as Figure 6. Notice that equivalent closed-loop damping in the targeted modes results in nearly identical responses.

To allow comparison of the control effort, in each case the closed loop system was subjected to a slew maneuver of the spacecraft and the energy which would be required to drive electromechanical actuators was calculated. Figure 7 shows a graph of the energy required to drive the actuators versus the percentage of available passive damping in the system. Note that the energy requirements drop rapidly as the passive damping level increases from nominal, due to the fewer number sensors and actuators required.

Table 9 Required Number of Actuators for Percentages of Maximum Achievable Damping

PERCENT OF MAXIMUM ACHIEVABLE DAMPING	NUMBER OF ACTUATORS REQUIRED
0	9
10	9
20	6
30	6
40	5
50	5
60	4
70	3
80	2
90	2
100	2

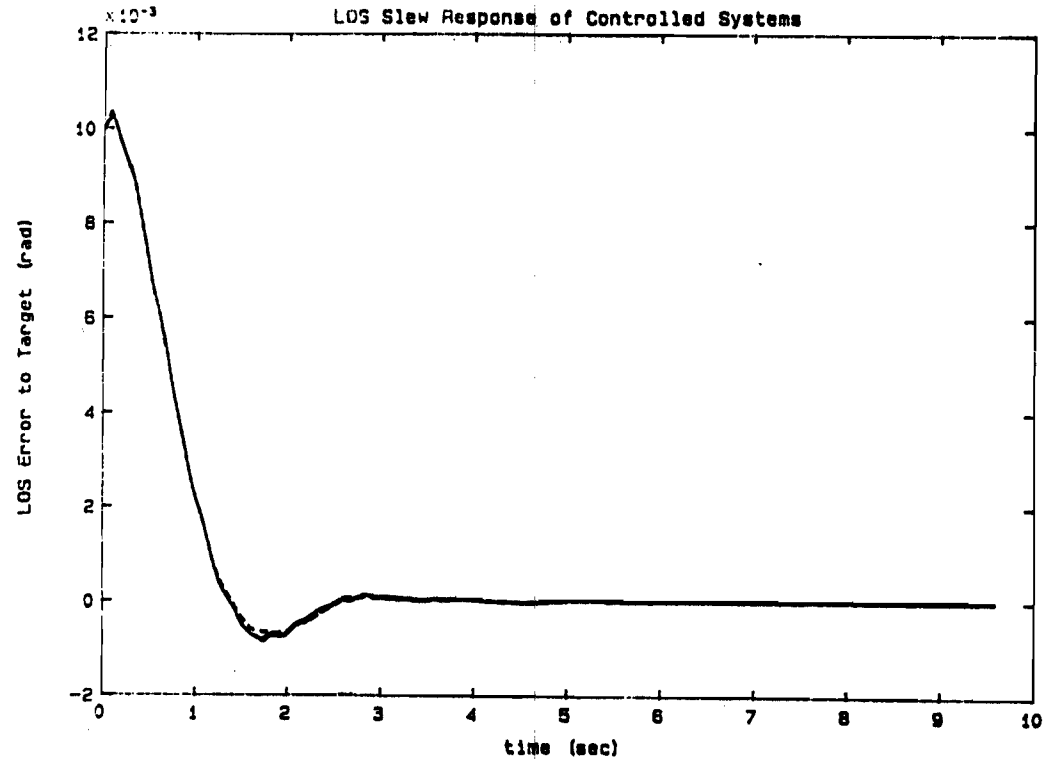

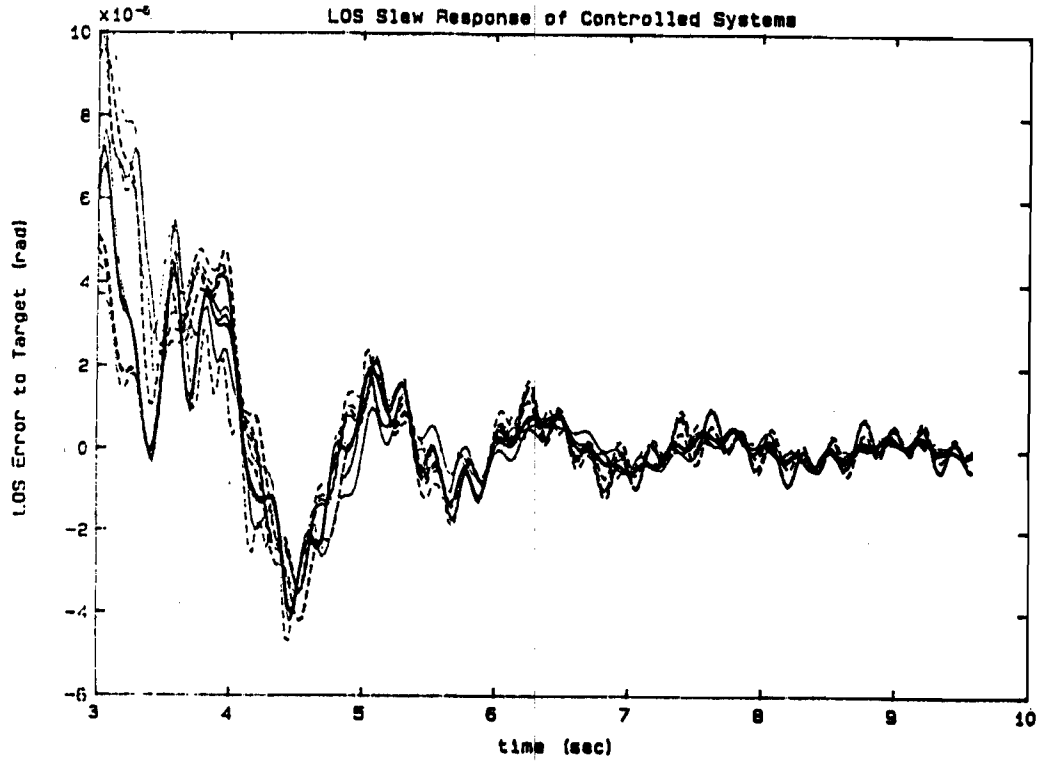

Figure 6 - LOS Slew Responses of Controlled Systems

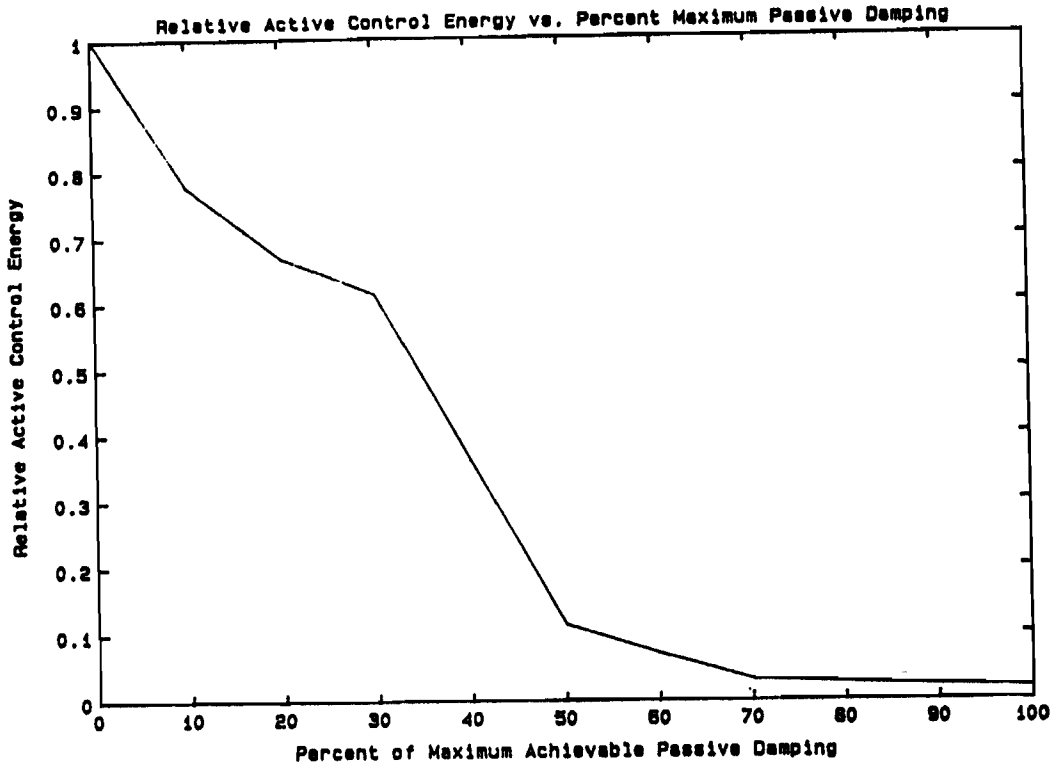

Figure 7 - Active Control Energy for Percentages of Achievable Passive Damping

As noted previously, spillover into modes not considered in the gain calculation affects the performance of the modal space control approach. This accounts for some of the higher energy requirements of the active system for low passive levels. For the control system for the undamped structure, three modes not intended to receive active damping augmentation were overdamped while several controlled modes did not have damping levels equal to the required values until the gains were adjusted iteratively. This can be interpreted as an inefficient use of control energy in that control effort is used to control modes of little importance to system performance. Use of a more sophisticated control algorithm and more sensors and actuators would reduce the spillover effects, but would be more sensitive to modeling errors and could lead to instabilities.

Selection of a Mix of Passive and Active Control

Using the results of the previous analyses, a mix of passive and active damping components was selected. A reasonable selection of the mix of the active and passive components was made on the basis of Figure 7 and Table 7.

Figure 7 shows a rapid decrease in the power required by the active control system as the percentage of available passive damping is increased from

nominal. At approximately 75% of the potential passive damping, the benefits of lower power requirements for the active system as passive level increases show diminishing returns. This can be seen by examining the maximum achievable damping on Table 7, and noting that at 75% of maximum all modes except 23 and 30 reach their design damping value. At this passive level, only the two sensor/actuator pairs were required, the control gains had acceptable values, and achieving the desired passive level would seem to be a relatively easy task. An important observation is that these damping levels correspond to achieving at least the target damping levels in all target modes except 23 and 30 and augmenting the damping of modes 23 and 30 actively.

Passive Damping Treatment Design

The passive damping analysis included design of the discrete damping devices to be used in the box truss and equipment platform structures; and the constrained layer treatments for the tripod legs, antenna support legs, and solar array hinges. The design process also included selection of the damping member locations for the box truss and equipment platform, and locations for the constrained layer treatments.

Table 7 shows that very high damping levels may be achieved in several modes with high box truss participation, damping levels which are not required for the system to meet the performance goals. The table also shows that the equipment platform dampers do not contribute damping levels sufficient to meet the performance goals for modes 23 and 30, but contribute more than enough damping to damp other modes to the required level. This implies that neither all the box truss or equipment platform diagonals need be damped. The number of diagonals selected in these two components were only those required to meet the design damping levels for the targets other than modes 23 and 30. Similarly, constrained layer treatments were applied only as required. The goal in subsequent damping design was therefore to achieve the design levels given in Table 6 for all target modes excluding modes 23 and 30 passively, and then to augment these two modes with an active system to their selected damping design values.

The designs of the discrete damping devices used on the RSA are very similar to the designs used used for corresponding elements on the PACOSS DTA. The extensional shear damper design used for the DTA box truss includes a spring between two relatively stiff damper support rods, and a section of viscoelastic wrapped around each rod and connected in parallel with the spring through a stiff clamshell. The design process for members of this type is discussed in several Reference 4. This design process was used to achieve a damper design with a high damping efficiency factor. Damped member weight was then calculated based on the member dimensions and materials. The final damper design corresponds to an approximate mass of 0.94 kg versus the original RSA box truss diagonal mass of 0.11 kg. The design damping efficiency of the box truss damper was 85%.

The locations for the dampers were selected from the strain energy distributions of the target modes. The number of damping locations was

selected such that the damping goals in all the target modes with high box truss participation were achieved with a minimum number of devices. The number of dampers required for the box truss was 40 members, of a total of 248 diagonals. The total mass of the box truss component was previously 2295 kg. Damping treatments add to this by approximately 1.6%.

The design of the extensional shear dampers for the equipment platform was very similar to that used for the box truss. A single shear design was utilized which does not include the elastic center spring. This design allows for more weight efficient utilization of the damping material. The final equipment platform damper design has a mass of 0.079 kg as compared to the weight of the original diagonal member of 0.018 kg. The damping efficiency of these members was 90%. A total of 18 dampers were required in order to achieve the damping attributed to the equipment platform for the final design damping levels. This corresponds to a negligible increase in mass of the original equipment platform mass of 2634 kg.

Since the design of constrained layer treatments for the tripod and antenna legs would be performed using solid elements and plate elements in MSC/NASTRAN, the actual design and analysis of these treatments was not performed due to cost and schedule constraints. A refined approximation of the damping effect and additional weight of the components due to these treatments was calculated based on the damping efficiency and relative thicknesses of the viscoelastic materials and constraining layers applied the DTA tripod legs.

The final dimensions and damping material for the treatment of the DTA tripod legs was a 0.050 in. thick acrylic core foam layer with a graphite epoxy constraining layer 0.050 in. thick applied to the legs which had a wall thickness of 0.065 in. This size relationship was used for the final estimates of all RSA constrained layer treatment performance. This treatment had a damping efficiency factor of approximately 17%. It should be noted that this design was in no way optimized on the DTA, so that the same damping efficiency may be achievable with lower relative VEM and constraining layer thicknesses.

Review of the strain energy distribution in the RSA tripod indicated that it was not necessary to damp the full length of the tripod legs. The major portion of the tripod leg strain energy was located toward the tripod apex in modes with significant tripod participation. This allowed only the upper three-fifths of the tripod legs to be treated in order to meet the target damping levels for these modes.

Similarly, the strain energy distribution in modes with antenna participation showed that only half of each antenna leg (half toward ring truss) required a constrained layer treatment. It was also determined that all the solar array hinges required treatment.

The final passive damping ratios of the RSA were calculated using the strain energy distribution for the treated elements in the final design (Table 10), the design damping efficiencies (Table 11), and the value for the loss

factor of acrylic core foam tape at 1.0 Hz and 70°F (0.73). This leads to final passive damping levels as given in Table 3-12.

To estimate the additional mass due to the constrained layer treatments, each treatment was considered to have the relationship that the constraining layer and viscoelastic material were each 77% as thick as the wall of the structural member to be treated, as in the DTA tripod design. Using this relationship and the densities of the structural and viscoelastic material, the added mass due to the constrained layer treatments was then calculated.

Table 13 contains a comparison of the system mass properties prior to the passive damping treatment application, and the estimated mass properties of the structure including damping treatments. Notice that the mass of the damping treatments is only a small percentage of the total system mass. A further benefit of the constrained layer damping treatments should be noted, however. Application of constrained layer treatments typically stiffens the structure, thereby increasing the system natural frequencies and lowering response levels. If identical natural frequencies were desireable, less added weight would be required for these treatments.

Table 10 - Strain Energy Percentages in Treated Elements for Final Design

		Percent Strain Energy in Treatments				
Mode No.	Freq. (Hz)	40 Box Truss Diagonals	3/5 of Tripod Legs	18 Equip Plat Diagonals	1/2 Antenna Legs	All Solar Array Hinges
23	0.73	-	2.37	1.03	45.9	3.46
30	1.02	-	1.43	5.32	22.7	20.7
32	1.03	-	-	1.73	5.17	66.5
48	1.53	-	6.01	4.06	7.12	7.74
124	2.8	5.62	59.9	-	2.24	0.6
129	2.9	57.1	2.34	0.08	-	-
158	4.0	7.25	17.4	-	3.86	-
165	4.2	1.09	56.7	-	1.33	-
182	4.5	3.19	52.2	-	-	-
185	5.1	7.96	1.77	-	12.6	-
187	5.7	20.6	19.7	-	1.29	-
191	6.5	1.88	1.30	30.4	4.77	-
196	7.0	47.5	2.65	1.10	-	-
198	7.1	26.9	11.8	-	3.02	-
199	7.3	18.0	2.0	-	-	-
201	7.4	8.60	48.3	8.01	1.51	-
206	8.8	31.5	24.0	1.17	2.78	-
209	9.4	34.4	-	-	-	-

Table 11 - Damping Efficiencies for Final Passive Damping Calculations

BOX TRUSS DAMPERS	TREATED TRIPOD LEGS	EQUIPMENT PLATFORM DIAGONALS	TREATED ANTENNA LEGS	TREATED SOLAR ARRAY HINGES
0.85	0.17	0.90	0.17	0.15

Table 12 - Damping Attributable to Component Treatments in Final Design

			Percent Modal Damping Attributable to Treatments					
Req'd. (%)	Mode No.	Freq. (Hz)	40 Box Truss Diagonals	3/5 of Tripod Legs	18 Equip Plat Diagonals	1/2 Antenna Legs	All Solar Array Hinges	Total
11.0	23	0.73	-	0.15	0.34	2.85	0.19	3.5
12.0	30	1.02	-	0.09	1.75	1.41	1.13	4.4
3.0	32	1.03	-	-	0.57	0.32	3.64	4.5
1.0	48	1.53	-	0.37	1.33	0.44	0.42	2.6
4.0	124	2.8	1.74	3.72	-	0.14	0.13	5.7
4.0	129	2.9	17.7	0.15	0.03	-	-	17.9
2.5	158	4.0	2.25	1.08	-	0.24	-	3.6
1.0	165	4.2	1.28	3.52	-	0.08	-	4.9
1.0	182	4.5	0.99	3.24	-	-	-	4.2
2.0	185	5.1	2.47	0.11	-	0.78	-	3.4
1.0	187	5.7	6.39	1.22	-	0.08	-	7.7
1.0	191	6.5	0.58	0.08	9.99	0.30	-	11.0
1.0	196	7.0	14.7	0.16	0.36	-	-	15.2
0.5	198	7.1	8.35	0.73	-	0.19	-	9.3
0.5	199	7.3	5.58	0.12	-	-	-	5.7
1.5	201	7.4	2.67	3.00	2.63	0.09	-	8.4
1.0	206	8.8	9.77	1.49	0.38	0.17	-	11.8
1.5	209	9.4	10.7	-	-	-	-	10.7

Table 13 - Estimated Mass Change Due to Damping Treatments

SUBSTRUCTURE	ORIGINAL MASS (kg)	CHANGE DUE TO TREATMENT MASS (kg)	% COMPONENT MASS CHANGE
Box Truss	2295	35.9	1.56
Ring Truss	1113	-	-
Tripod	840	227	27.0
Equipment Platform	2634	1.10	0.0
Antenna	345	71	21.0
Solar Arrays	786	13.2	1.68
SYSTEM	8013	348	4.3

The active control algorithm was used to provide additional damping to modes 23 and 30 for the final passive design. The final open and closed loop frequencies and damping ratios for the passive/active RSA design are listed in Table 14. This table shows that although spillover effects were present for the passively damped system, they are far less severe than observed with only nominal passive damping. Notice that the required damping ratios with a 1.5 factor of safety have been achieved by passive damping in the modes which were the original targets; excluding modes 23 and 30 which have their target levels achieved through a combination of passive and active damping.

Table 15 contains a summary of the mass properties of several candidate actuators which could be used for the active control system. For the active-alone system, the maximum torques required from the actuators during the slew maneuver were calculated and are included in Table 16. Notice that high torques are required of several actuators. Selecting the actuators which can produce the required torques and have minimum mass, the additional system mass due to the actuators is given in Table 17. Actuators which are in symmetric pairs were given the mass properties of a single actuator, but the actual implementation is two actuators each producing one half the torque on Table 16. The inclusion of only one actuator mass assumes that there exists actuators of one half the mass of the Bendix MA 500 actuators which can produce one half the torque.

The actuator data indicates that in order to achieve the necessary active control authority for the active-alone system, two Sperry 600 actuators and seven Bendix MA 500 actuators were needed. The mass associated with this hardware has a total of 620 kg. The maximum torques required for the two actuators in the passive/active system were also calculated and are included in Table 18. The passive/active system would therefore require two Bendix MA 500 actuators along with the passive damping treatments.

Table 14 - Open and Closed-Loop Frequencies and Damping for Final Passive/Active System

SYSTEM	OPEN LOOP		CLOSED LOOP	
MODE #	f_n (Hz)	ζ (%)	f_n (Hz)	ζ (%)
Rigid Body	0	0	0.45	59.7
Filter	1.0	70.7	0.55	82.7
7	0.01	0.2	0.50	70.63
21	0.69	0.2	0.69	0.33
* 23	0.73	3.5	0.80	11.63
* 30	1.02	4.4	0.96	13.70
32	1.02	4.5	1.02	4.52
44	1.50	0.2	1.50	0.53
48	1.53	2.6	1.56	14.29
118	2.72	0.2	2.72	0.21
124	2.78	5.7	2.78	6.57
129	2.86	17.9	2.88	18.45
158	4.03	3.6	4.05	4.71
165	4.21	4.9	4.21	5.40
176	4.38	0.2	4.38	0.21
182	4.55	4.2	4.55	4.26
185	5.11	3.4	5.13	7.30
187	5.68	7.7	5.67	8.41
188	5.81	0.2	5.81	0.23
191	6.45	11.0	6.11	81.41
192	6.49	0.2	6.45	4.30
196	6.96	15.2	6.95	15.14
198	7.15	9.3	7.14	9.56
199	7.31	5.7	7.28	6.00
201	7.38	8.4	7.32	8.14
206	8.77	11.8	8.75	12.46
209	9.53	10.7	9.53	10.71

*Denotes active control target mode

Table 15 - Control Moment Gyro Characteristics

Mfr	Model No.	Gimbal Type	Angular Momentum N-m-s	Angular Momentum ft-lb-s	Rate (r/min)	Torque (N-m)	Torque (ft-lb)	Weight (lb)	Envelope (in.)	Design Status	Applications
Bendix	MA 5-100-1	Double	6.78	5	8,000	135.6	100	38	10 dia X 10	Lab prototype	LAPSO pointer prototype
Bendix	MA 500 AC	Single	399-1,017	250-750	7,850	678	500	145	20 dia X 32	Experimental	
Bendix	MA 500 DC	Single	399-1,017	250-750	7,850	678	500	155	20 dia X 32		
Bendix	MA 1000	Double	1,356	1,000	11,400	237.3	175	230	39 dia sphr	Experimental	NASA — Langley
Bendix	MA 2300	Double	3,119	2,300	9,000	165.4	122	418	49 dia sphr		Skylab
Bendix	MA 2000	Double	1,356-4,068	1,000-3,000	4,000-12,000	237.3	175	558	44 dia sphr	Advanced development Skylab unit	
Sperry	30	Double	40.7	30	4,750	6.8	5 (pk)	32	22 dia X 12	Prod	COMSAT/TRW
Sperry	75	Double	102	75	4,000	3.0	2.2 (pk)	48	20 dia X 10	Prod	COMSAT
Sperry	100	Single & double	136	100	8,000			48		Experimental unit	
Sperry	150	Single	203	150							
Sperry	400	Single		400							
Sperry	600	Single	676-1,356	500-1,000	3,000-6,000	1,356	1,000	175	31 X 41 X 33		
Sperry	1200	Single	813-2,712	600-2,000	2,810-6,700	2,712	2,000	200	31 X 41 X 23		
Sperry	4500	Double	6,101	4,500	6,500		200	500	48 X 48 dia	Experimental	NASA — Langley (Space Station Res)

Ref: CSDL-R-1499, An Investigation of Enabling Technologies for Large Precision Space Systems, September 1982, Vol. 3: R. Strunce, et. al.

3383-73
268.327-63

Table 16 - Maximum Torques Required from Actuators Using Active Control Alone

ACTUATOR #	MAXIMUM TORQUE (N-m)
1	936
2	1371
3	633
4	520
5	261
6	226
7	212
8	475
9	106

Table 17 - Actuator Types Selected for Active Control Alone System and Associated Mass Properties

ACTUATOR #	ACTUATOR TYPE	MASS (kg)
1	Sperry 600	79.5
2	Sperry 600	79.5
3	Bendix MA 500 DC	65.9
4	Bendix MA 500 DC	65.9
5	Bendix MA 500 DC	65.9
6	Bendix MA 500 DC	65.9
7	Bendix MA 500 DC	65.9
8	Bendix MA 500 DC	65.9
9	Bendix MA 500 DC	65.9
	TOTAL	620.3

Table 18 - Maximum Torques Required from Actuators for Passive/Active Design

ACTUATOR #	MAXIMUM TORQUE (N-m)
1	167
2	136

Table 19 - Mass Properties Associated with Damping Devices in Passive/Active Final Design

DESCRIPTION	MASS (kg)
Passive Treatments	348
Actuator 1 (Bendix MA 500 DC)	65.9
Actuator 2 (Bendix MA 500 DC)	65.9
TOTAL	479.8

The total mass associated with passive and active control damping devices for the passive/active system would then be 480 kg as shown in Table 19. The additional mass of the passive/active system is 140 kg less than the mass associated with the actuators for the active control alone design. This mass comparison does not include any additional weight which may be required to eliminate outgassing or control temperature of the viscoelastic for the passive damping treatments, but these will most likely be small compared to the 140 kg difference between the two designs. The active control added mass estimate includes only actuator masses and not any additional mass for electronics required to operate the control system, or additional power or fuel needs.

The energy requirements of the active and passive/active systems can be compared by examination of Figure 7. The relative electrical energy required to drive the actuators for the passive/active system is less than 3.0% of that required for the active-alone system (this roughly corresponds to 75% maximum achievable damping on Figure 7). The actual comparison calculated from the slew maneuver of the final damped design is 2.6%. The passive/active system therefore has much lower requirements for a power source to drive the actuators. Of course, energy required for temperature control of the passive damping treatments, if necessary, should also be included in this comparison. Proper insulation and shielding of the treatments would probably make this power negligible.

It should be noted that in the previous comparison, the assumptions are biased in favor of the active components in the calculations. A damping factor of safety was used for the passive damping component in the final design, as the passive damping in the target and observable modes for the final design was at least 50% above the required value in each case. The active control damping component was allowed to achieve only slightly higher than the required damping levels in the target modes, although significant damping was obtained in several observable modes due to spillover. No factors of safety or gain margins were considered in the active control design.

The mass comparison of the two designs included only the mass of the actuators used for active control, while the larger power requirements of the active-alone system would surely result in a more massive power supply. Any additional wiring required for the larger number of sensors and actuators should also be included in the mass calculations, but was not. Also, control system electronics and redundant components which would be required for the active system were not included in the mass calculations.

Perhaps the largest effects not accounted for in the comparison were the effects on the modal parameters of the addition of the actuators and passive damping treatments. While the effects of the discrete box truss and equipment platform dampers on mode shapes and frequencies would be small, the addition of the constrained layer treatments to the tripod, antenna, and solar arrays would result in higher frequencies for the target modes since the structure would be stiffened in locations which have high strain energy in these modes. Alternatively, the addition of the large masses of the actuators at points of high modal deflections in the target modes (such as

at the equipment platform or antenna tips) would result in much lower frequencies since these masses would then have high generalized mass contributions. These effects would result in increased damping requirements for the active-alone system and decreased damping requirements for the passive/active system.

Conclusions

From the comparison of the active-alone system and the passive/active system, and the results of the RSA study, several conclusions may be drawn. These are:

1) Passive damping and/or active control will provide dramatic improvement in the performance of future space systems. For the RSA, a factor of 230 improvement in settling time after the slew maneuver was achieved.

2) Passive damping will be required for efficient implementation of vibration control technology on future space systems.

3) The passive/active RSA vibration control system, as compared to the active-alone RSA system, has much lower power requirements, higher reliability, lower active control system gains, and fewer electronic components.

4) Lower weight for overall systems will result from consideration of passive and active control together in an integrated damping methodology.

5) The fewer number of electronic components, lower overall weight and lower system power requirements of the passive/active system compared to the active-alone system are indicative of lower overall system costs.

Acknowledgement

This work was supported by the Air Force Wright Laboratories under the Passive and Active Control of Space Structures (PACOSS) program, contract number F33615-82-C-3222.

References

1. Morgenthaler, D. R. and Gehling, R. N., "Design and Analysis of the PACOSS Representative System," Damping 1986 Proceedings, May 1986 (AFWAL-TR-86-3059, Vol. 2), pp. DG-1-DG-31.

2. Gehling, R. N., "Active Augmentation of a Passively Damped Representative Large Space System," Damping 1986 Proceedings, May 1986, (AFWAL-TR-86-3059, Vol. 2), pp. EB-1-EB-18.

3. Gehling R. N., "Low Authority Control Through Passive Damping," Presented at the Annual AAS Guidance and Control Conference, Keystone, CO, February 1-5, 1986 (AAS 86-004).

4. Morgenthaler, D. R., "Design and Analysis of Passively Damped Large Space Structures," Presented at the 11th ASME Biennial Conference on Mechanical Vibration and Noise, Boston, Massachussetts, 27-30 September, 1987, (DE-Vol. 5), pp. 1-8.